IAI Journals.ASM.org

Intestinal Epithelium-Specific MyD88 Signaling Impacts Host Susceptibility to Infectious Colitis by Promoting Protective Goblet Cell and Antimicrobial Responses

Ganive Bhinder, Martin Stahl, Ho Pan Sham,* Shauna M. Crowley, Vijay Morampudi, Udit Dalwadi, Caixia Ma, Kevan Jacobson, Bruce A. Vallance

Division of Gastroenterology, Department of Pediatrics, Child and Family Research Institute, University of British Columbia, Vancouver, British Columbia, Canada

Intestinal epithelial cells (IECs), including secretory goblet cells, form essential physiochemical barriers that separate luminal bacteria from underlying immune cells in the intestinal mucosa. IECs are common targets for enteric bacterial pathogens, with hosts responding to these microbes through innate toll-like receptors that predominantly signal through the MyD88 adaptor protein. In fact, MyD88 signaling confers protection against several enteric bacterial pathogens, including *Salmonella enterica* serovar Typhimurium and *Citrobacter rodentium*. Since IECs are considered innately hyporesponsive, it is unclear whether MyD88 signaling within IECs contributes to this protection. We infected mice lacking MyD88 solely in their IECs (*IEC-Myd88*$^{-/-}$) with *S.* Typhimurium. Compared to wild-type (WT) mice, infected *IEC-Myd88*$^{-/-}$ mice suffered accelerated tissue damage, exaggerated barrier disruption, and impaired goblet cell responses (Muc2 and RELMβ). Immunostaining revealed *S.* Typhimurium penetrated the IECs of *IEC-Myd88*$^{-/-}$ mice, unlike in WT mice, where they were sequestered to the lumen. When isolated crypts were assayed for their antimicrobial actions, crypts from *IEC-Myd88*$^{-/-}$ mice were severely impaired in their antimicrobial activity against *S.* Typhimurium. We also examined whether MyD88 signaling in IECs impacted host defense against *C. rodentium*, with *IEC-Myd88*$^{-/-}$ mice again suffering exaggerated tissue damage, impaired goblet cell responses, and reduced antimicrobial activity against *C. rodentium*. These results demonstrate that MyD88 signaling within IECs plays an important protective role at early stages of infection, influencing host susceptibility to infection by controlling the ability of the pathogen to reach and survive at the intestinal mucosal surface.

Each year, enteric infections cause more than 1.5 billion cases of diarrheal disease, along with more than 2 million deaths (1). Many of these cases reflect infection by bacterial pathogens such as *Salmonella enterica* serovar Typhimurium and enteropathogenic *Escherichia coli* (EPEC) (1, 2). Although bacterial virulence factors play a significant role in determining whether an infection is successful, the host's innate immune response also plays an integral role in determining its overall susceptibility to infection, as well as regulating the course and severity of disease suffered during a successful infection. A significant aspect of the host's innate response to such infections is mediated by toll-like receptor (TLR) signaling pathways, most of which signal by recruiting the key adaptor protein myeloid differentiation factor 88 (MyD88) (3). Ligation of most TLRs by conserved microbe-associated molecular patterns, as well as interleukin-1 and -18 receptors (IL-1R and IL-18R, respectively), by their respective ligands results in recruitment of MyD88 to the receptor complex, initiating its activation and a cascade of signaling events leading to the activation of an array of inflammatory genes (3).

Although first recognized for its role in proinflammatory pathways, several studies in recent years have uncovered a critical protective role for MyD88 signaling in the promotion of mucosal homeostasis following inflammatory insult (4–11). This notion was first identified when Myd88-deficient (Myd88$^{-/-}$) mice were shown to be highly susceptible to dextran sodium sulfate (DSS)-induced colitis (4). MyD88 signaling was found to play a key protective role, promoting the production of tissue protective factors and the increased proliferation of IECs during colitis, with mice lacking MyD88 suffering widespread mucosal tissue damage and ulceration. Later work by our group and others found that MyD88 also played an essential protective role during the infectious colitis caused by the natural murine pathogen *Citrobacter rodentium* (5, 6), a close relative of EPEC (12).

Bone marrow transplantation studies have shown that the protective effects of MyD88 during colitis reflect signaling in both the hematopoietic and the nonhematopoietic cell compartments (6, 10, 11). While many of the MyD88-dependent changes that prove protective during colitis reflect changes in intestinal epithelial cell (IEC) function and/or proliferation, it remains uncertain whether any of the protective signaling occurs within the IECs themselves. Considering that the IEC layer is in constant contact with commensal microbes, these cells are known to be innately hyporesponsive to most bacterial products as a way to prevent overt spontaneous inflammatory responses against commensal microbes (13–15). In fact, several groups have studied the specific role of MyD88 signaling in IECs during DSS-induced colitis, and most, but not all, studies found little evidence for its involvement (9, 16). Correspondingly, in a recent study where we examined

Received 12 May 2014 **Returned for modification** 1 June 2014
Accepted 14 June 2014
Published ahead of print 23 June 2014
Editor: A. J. Bäumler
Address correspondence to Bruce A. Vallance, bvallance@cw.bc.ca.
* Present address: Ho Pan Sham, Pulmonary and Critical Care Medicine Division, Brigham and Women's Hospital, Boston, Massachusetts, USA.

doi:10.1128/IAI.02045-14

whether IECs played any role in responding to *C. rodentium* infection, we found no evidence that *IEC-Myd88*$^{-/-}$ mice were more susceptible to infection than wild-type (WT) mice, although in this study we focused solely on later stages of infection (15).

Considering that innate signaling within IECs might have a greater impact at early stages of infection, prior to the recruitment of large numbers of inflammatory cells, we decided to reexamine the role of MyD88 signaling in IECs. Therefore, we infected WT and *IEC-Myd88*$^{-/-}$ mice with the enteric pathogens *S.* Typhimurium and *C. rodentium* and examined responses at very early time points. We found that the loss of MyD88 signaling in IECs increased early susceptibility to infection, impairing the induction of several key antimicrobial genes as well as the expression of the goblet cell (GC)-specific factors Resistin-like molecule beta (Relmβ) and mucin 2 (Muc2) during infection. Correspondingly, the bactericidal activity of crypt supernatants from *IEC-Myd88*$^{-/-}$ mice was significantly reduced against both *S.* Typhimurium and *C. rodentium* compared to that of crypts isolated from WT mice. This impairment in antimicrobial defenses appears to facilitate the ability of these bacterial pathogens to reach and infect the intestinal epithelium, resulting in accelerated intestinal tissue damage and barrier dysfunction. Thus, our study demonstrates that MyD88 signaling in the intestinal epithelium *in vivo* confers protection to the host at the initial stages of an enteric bacterial infection.

MATERIALS AND METHODS

Mice. *MyD88 flox/flox* mice and Villin-cre mice (all on a C57BL/6 genetic background) were purchased from The Jackson Laboratory. *IEC-Myd88*$^{-/-}$ mice were generated by crossing *MyD88 flox/flox* mice with Villin-cre mice, and the resulting litters were genotyped. *MyD88 flox/flox* mice were used as wild-type controls for all studies. All mice were kept in sterilized, filter-topped cages and fed autoclaved food and water under specific-pathogen-free conditions at the Child and Family Research Institute (CFRI). The protocols employed were approved by the University of British Columbia's Animal Care Committee and were in direct accordance with guidelines provided by the Canadian Council on the Use of Laboratory Animals.

Bacterial strains and infection of mice. The *Salmonella* Typhimurium SL1344 Δ*aroA* mutant (17) and streptomycin-resistant *Citrobacter rodentium* DBS100 (formerly *C. freundii* biotype 4280, strain DBS100) strains were grown with shaking (200 rpm) at 37°C in Luria-Bertani (LB) broth supplemented with 100 μg/ml streptomycin. Twenty-four h prior to SL1344 Δ*aroA* mutant infection, 6- to 10-week-old mice were treated with 20 mg of streptomycin (in 100 μl) by oral gavage. Mice were infected with 3×10^6 CFU of *Salmonella* in 100 μl phosphate-buffered saline (PBS) buffer (pH 7.2) by oral gavage. Mice infected with *C. rodentium* were inoculated by oral gavage with 100 μl of overnight culture (~2.5×10^8 CFU).

Tissue collection and bacterial counts. Mice were anesthetized with isoflurane and euthanized via cervical dislocation at various time points over the course of infection. For bacterial cell counts, the cecum, colon, and luminal contents each were collected and homogenized separately in 1 ml of sterile PBS. Samples were serially diluted and plated on streptomycin-supplemented LB agar plates and incubated at 37°C overnight, and colonies were enumerated and normalized to the weight of the tissues. For histology, cecal samples were fixed in 10% neutral buffered formalin (Fischer Scientific) overnight, transferred to 70% ethanol, embedded in paraffin, and cut into 5-μm sections.

Histology scoring. Five-μm tissue sections were stained with hematoxylin and eosin (H&E) (by the histology laboratory at the CFRI) and were examined by two blinded observers to assess histological damage. Tissue sections were assessed for (i) submucosal edema (0, no change; 1, mild; 2, moderate; 3, severe); (ii) hyperplasia (0, no change; 1, 1 to 50%; 2, 51 to 100%; 3, >100%); (iii) goblet cell depletion (0, no change; 1, mild depletion; 2, severe depletion; 3, absence of goblet cells); (iv) epithelial integrity (0, no pathological changes detectable; 1, epithelial desquamation [a few cells sloughed, surface rippled]; 2, erosion of epithelial surface [epithelial surface rippled, damaged]; 3, epithelial surface severely disrupted/damaged, large amounts of cell sloughing; 4, ulceration [with an additional score of 1 added for each 25% of tissue in the cross-section affected, e.g., a large ulcer affecting 70% of the tissue section would be scored 4 + 3]); (v) mucosal mononuclear cell infiltration (per ×400 magnification field) (0, no change; 1, <20; 2, 20 to 50; 3, >50 cells/field); and (vi) submucosal polymorphonuclear leukocytes (PMN) and mononuclear cell infiltration (per ×400 magnification field) (1, <5; 2, 21 to 60; 3, 61 to 100; 4, >100 cells/field). The maximum possible score was 22.

Commensal microbe analysis. Microbial composition analysis was performed by quantitative PCR (qPCR) as described previously (18). DNA was extracted from at least two fecal pellets per animal using the Qiagen DNA stool extraction kit. Fifty ng of extracted DNA per reaction was used for qPCR. 16S rRNA group-specific primers were used to determine the relative abundance of the selected bacterial phyla: *Bacteroidetes* (5′-GAG AGG AAG GTC CCC CAC-3′ and 5′-CGC TAC TTG GCT GGT TCA G-3′) (19), *Firmicutes* (5′-GGA GYA TGT GGT TTA ATT CGA AGC A-3′ and 5′-AGC TGA CGA CAA CCA TGC AC-3′) (20), and *Gammaproteobacteria* (5′-TCG TCA GCT CGT GTY GTG A-3′ and 5′-CGT AAG GGC CAT GAT G-3′) (21). Universal *Eubacteria* primers (5′-ACT CCT ACG GGA GGC AGC AGT-3′ and 5′-ATT ACC GCG GCT GCT GGC3′) (22) were used to determine total bacterial 16S rRNA in each sample, and the relative abundance of each taxonomic group was determined by calculating the average threshold cycle (C_T) value relative to this number, normalized to each primer's determined efficiency.

FITC-dextran intestinal permeability assay. The fluorescein isothiocyanate (FITC)-dextran intestinal permeability assay was performed as previously described (15). Uninfected mice or mice at day 1 (D1), D3, or D4 postinfection (pi) were gavaged with 150 μl of 80 mg/ml 4-kDa FITC-dextran (Sigma-Aldrich) in PBS 4 h prior to sacrifice. Mice were anesthetized, and blood (~500 μl) was collected by cardiac puncture and added immediately to a final concentration of 3% acid-citrate dextrose (20 mM citric acid, 100 nM sodium citrate, 5 mM dextrose). The FITC-dextran concentration in serum was measured using a fluorometer (Perkin-Elmer Life Sciences) (excitation wavelength, 485 nm; emission wavelength, 530 nm).

RNA extractions and quantitative real-time PCR. Immediately following euthanization of mice, cecal tissues were placed in RNAlater (Qiagen) and stored at −80°C. Total RNA was extracted using a Qiagen RNeasy kit according to the manufacturer's instructions. Total RNA was quantified using a NanoDrop spectrophotometer, and cDNA was synthesized using 1 μg of RNA with an Omniscript reverse transcription (RT) kit (Qiagen). For the qPCR reaction, 5 μl of a 1:5 dilution of cDNA was added to 10 μl Bio-Rad SYBR green supermix with primers (final concentration, 300 nM; final volume, 20 μl), and qPCR was carried out using a Bio-Rad MJ MiniOpticon machine. Quantitation of data was carried out using Gene Expression Macro OM 3.0 software (Bio-Rad).

Immunohistochemistry. Five-μm paraffin sections were deparaffinized by heating to 60°C for 15 min, cleared with xylene, rehydrated through an ethanol gradient to water, and steamed for 30 min in citrate buffer for antigen retrieval. Tissues then were blocked using blocking buffer (goat or donkey serum in PBS containing 1% bovine serum albumin [BSA], 0.1% Triton X-100, 0.05% Tween 20, and 0.05% sodium azide). The primary antibodies used were anti-Muc2, anti-Relmβ, anti-Ki-67, anti-*Salmonella* lipopolysaccharide (LPS), anti-β-actin, and anti-Tir, and the secondary antibodies were Alexa Fluor 568- or 488-conjugated goat anti-rabbit and goat anti-rat IgG and Alexa Fluor 568- or 488-conjugated donkey anti-rabbit or donkey anti-goat IgG. ProLong gold antifade reagent with 4′,6-diamidino-2-phenylindole (DAPI; Invitrogen) to stain DNA was used to mount tissues. Tissues were viewed on a

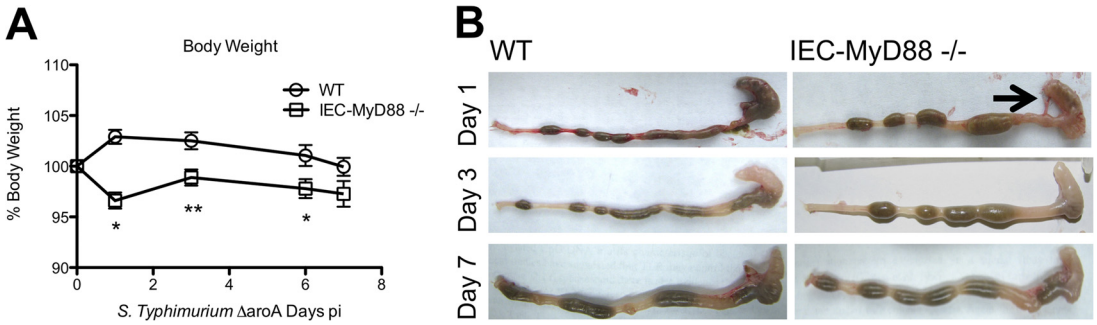

FIG 1 *IEC-Myd88*$^{-/-}$ mice are more susceptible to *S.* Typhimurium-induced colitis. (A) Body weights of WT and *IEC-Myd88*$^{-/-}$ mice from D0 to D7 pi, plotted as a percentage of starting weight. *IEC-Myd88*$^{-/-}$ mice exhibited rapid weight loss by D1 pi that remained significantly below that of WT mice until D6 pi. (B) Unlike WT mice, at D1 pi the *IEC-Myd88*$^{-/-}$ intestinal tissues displayed severe damage, with severely shrunken ceca devoid of stool contents. The black arrow indicates inflamed ceca, and error bars indicate SEM from at least 6 mice. *, $P < 0.05$; **, $P < 0.005$.

Zeiss Axio Imager microscope, and images were taken using AxioVision software and an AxioCam HRm camera.

Fluorescence intensity measurements. The fluorescence intensity of immunostained samples was assessed using ImageJ software to determine the ratio of Muc2 or Relmβ in each tissue section to DAPI staining. This was done using the integrated density measurement tool. Integrated density for each image was assessed on separate channels to determine the pixel intensity of DAPI and Muc2 or Relmβ for each section. The fluorescence intensity then was represented as the integrated density value of Muc2 or Relmβ relative to total DAPI integrated density values.

Crypt-killing assay. As described previously (15, 23), cecal and colonic crypts were isolated from uninfected WT (C57BL/6) and IEC-*Myd88*$^{-/-}$ mice. Ceca and colons were extracted from mice following euthanization and placed in 50 μg/ml gentamicin in sterile PBS following removal of fecal contents. Tissues were washed 3× in the gentamicin-PBS solution, cut into small (0.5-cm) sections, and placed in a petri dish containing 10 ml of BD cell recovery solution at 4°C for 2 h. Crypts then were dislodged by gently flicking with forceps in the dish. Following centrifugation, crypts were resuspended in iPIPES buffer [10 mM piperazine-*N*,*N*′-bis(2-ethanesulfonic acid) (PIPES), pH 7.4, 137 mM NaCl] at 2,000 crypts per 40 μl buffer and incubated at 37°C for 30 min. Samples then were centrifuged, and supernatant was collected. Eleven μl of supernatant was added to 10^3 *S.* Typhimurium Δ*aroA* mutant cells, 10^3 *C. rodentium* cells, or 20 μM RegIII-γ as a positive control and incubated at 37°C for 2 h. Antimicrobial activity was assessed by counting overnight growth of crypt supernatant-treated *S.* Typhimurium Δ*aroA* mutant or *C. rodentium* and expressed as percent bacterial growth relative to overnight growth observed in cultures treated with sterile iPIPES alone.

Statistical analysis. All results presented in this study are expressed as the mean values ± standard errors of the means (SEM). Nonparametric Mann-Whitney *t* tests or Student's *t* tests were performed using GraphPad Prism software, version 5.00, for Mac. A *P* value of 0.05 or less was considered significant.

RESULTS

***IEC-Myd88*$^{-/-}$ mice suffer exaggerated *S.* Typhimurium-induced gastroenteritis.** To assess whether IEC-specific MyD88 signaling plays any role in regulating host defense and intestinal inflammation in response to *S.* Typhimurium, we infected *Myd88 flox/flox* (WT) and *IEC-Myd88*$^{-/-}$ mice with the *S.* Typhimurium Δ*aroA* mutant and assessed body weights over the ensuing 7 days. This *Salmonella* strain was chosen because it does not kill mice on a C57BL/6 genetic background, whereas it still causes severe gastroenteritis in infected mice (24, 25). Although 6- to 8-week-old WT and *IEC-Myd88*$^{-/-}$ mice displayed similar body weights (data not shown), infected WT mice showed an early weight gain at D1 to 3 pi, followed by modest weight loss, while *IEC-Myd88*$^{-/-}$ mice exhibited significantly greater (*, $P < 0.05$) weight loss (~5%) over the first 6 days of infection (Fig. 1A). Following their euthanization at specific time points, infected *IEC-Myd88*$^{-/-}$ mice showed greater macroscopic intestinal damage than WT mice, with severely shrunken ceca that were devoid of stool content as early as D1 pi (Fig. 1B).

As the majority of the pathology seen in this model occurred in the cecum, we focused our subsequent analysis on this region. At both D1 and D3 pi, *IEC-Myd88*$^{-/-}$ mice displayed significantly greater cecal histopathology scores than WT mice, represented by increased GC depletion, IEC damage, and inflammatory cell infiltration ($P < 0.001$) (Fig. 2A and B). Specifically, we noted the presence of more macrophages and neutrophils infiltrating the cecal tissues of the *IEC-Myd88*$^{-/-}$ mice, although infected WT and *IEC-Myd88*$^{-/-}$ mice showed similarly increased gene transcript levels for the chemokines MCP-1 and MIP-2α (Fig. 2C). While *IEC-Myd88*$^{-/-}$ mice showed decreased induction of gene transcript levels for the inflammatory cytokine tumor necrosis factor alpha (TNF-α) compared to WT mice, gamma interferon (IFN-γ), IL-1β, and IL-17A were induced to similar levels at D1 pi (*, $P < 0.05$) (Fig. 2C).

***IEC-Myd88*$^{-/-}$ mice show altered localization of *S.* Typhimurium within ceca.** As increased intestinal pathology often is associated with higher pathogen burdens during infection, we enumerated the *S.* Typhimurium Δ*aroA* mutant within cecal tissues and within the lumen, as well as in the spleen and liver tissues of mice at D1 and D3 pi. Surprisingly, no significant differences in pathogen burdens were found at any of these sites at either time point (Fig. 3A). Since exaggerated inflammation also could reflect deeper penetration of tissues by the pathogens, we next used immunostaining to visualize the location of *S.* Typhimurium within the intestine. Immunostaining for *Salmonella* LPS revealed that the majority of *S.* Typhimurium remained sequestered within the cecal lumen in WT mice, whereas in *IEC-Myd88*$^{-/-}$ mice, the *S.* Typhimurium organisms were found in close proximity to the epithelial surface, as outlined by staining for β-actin (Fig. 3B).

IEC-specific MyD88 signaling does not overtly alter the gut microbiome. Host susceptibility to enteric bacterial infections can be influenced by differences in the makeup of the intestinal microbiota. A recent study reported that the commensal microbe populations of *IEC-Myd88*$^{-/-}$ mice differed from that of WT mice under baseline conditions (16). While our pretreatment of

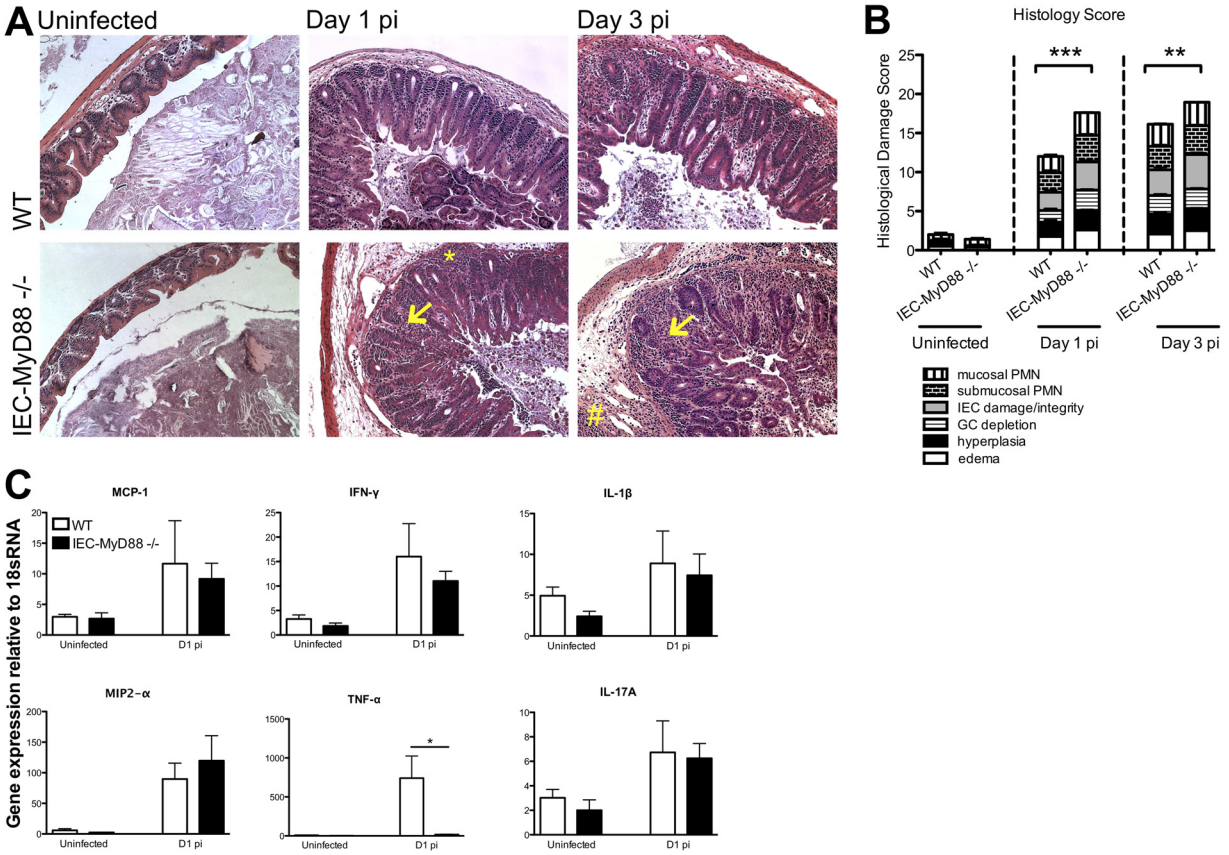

FIG 2 *IEC-MyD88*$^{-/-}$ mice suffer accelerated tissue damage during *S.* Typhimurium infection. (A) Representative H&E staining of cecal tissues from WT and *IEC-MyD88*$^{-/-}$ mice taken under uninfected conditions or at D1 and D3 pi. *IEC-MyD88*$^{-/-}$ mice exhibited increased edema, inflammatory cell infiltrate (*, mucosal infiltration; #, submucosal infiltration), and damage to IEC integrity (arrows) at D1 and D3 pi. (B) Comparative histological damage scores of uninfected and infected (D1 and D3 pi) *IEC-MyD88*$^{-/-}$ and WT mice. Cecal tissues of *IEC-MyD88*$^{-/-}$ mice displayed significantly higher histological damage scores at both D1 and D3 pi. Bars represent the damage scores from at least 3 experiments, each with 3 to 5 mice. Error bars indicate SEM. **, $P < 0.005$; ***, $P < 0.0005$. (C) Infected WT and *IEC-MyD88*$^{-/-}$ mice show similar increases in gene transcript levels for the chemokines MCP-1 and MIP2-α, as well as for IFN-γ, IL-1β, and IL-17A. In contrast, compared to WT mice, the *IEC-MyD88*$^{-/-}$ mice showed significantly decreased transcript levels for TNF-α after infection with the *S.* Typhimurium Δ*aroA* mutant. Results are representative of 3 independent infections. Original magnification, ×200.

mice with the antibiotic streptomycin likely minimized any impact of the microbiota in our infections, we decided to assess the intestinal microbiomes of the mice at our facility both pre- and poststreptomycin treatment. Using qPCR analysis of fecal pellets, we found that members of the phylum *Bacteroidetes* were the dominant commensals present under uninfected conditions in both groups (~50 to 70%), whereas smaller numbers of *Firmicutes* (~5 to 10%) and other bacteria represented the remainder of the commensals. There was a substantial shift in bacterial populations after streptomycin treatment at D1 pi, with significant decreases seen in both *Bacteroidetes* and *Firmicutes* and a significant increase in *Gammaproteobacteria* (~35 to 60%, likely largely representing *Salmonella*) in both WT and *IEC-Myd88*$^{-/-}$ mice (Fig. 3C). Despite modest differences in the exact percentages of the different phyla between WT and *IEC-Myd88*$^{-/-}$ mice, no overt/significant differences in commensals were noted between strains under uninfected conditions or poststreptomycin treatment, infected conditions (Fig. 3C).

MyD88 signaling in IECs protects barrier integrity during infection. Several previous studies have implicated MyD88-dependent signaling as driving profound protective changes in IEC proliferation and barrier function (4, 5) during infectious or chemically induced models of colitis. Moreover, defects in IEC responses could be responsible for the exaggerated cecitis suffered by the *IEC-Myd88*$^{-/-}$ mice. Therefore, we examined whether the barrier maintenance and increased IEC proliferation that develop during *S.* Typhimurium infection were mediated by MyD88 signaling within the IECs.

Following oral gavage of FITC-dextran, we found that IEC-specific MyD88 signaling had no effect on baseline barrier function, as serum FITC-dextran levels were similar in uninfected WT and *IEC-Myd88*$^{-/-}$ mice (Fig. 4A). In contrast, although the *S.* Typhimurium Δ*aroA* mutant was able to cause a modest impairment in epithelial barrier function in WT mice by D1 that lasted until D3 pi (*, $P < 0.05$), infected *IEC-Myd88*$^{-/-}$ mice demonstrated significantly greater (2-fold) intestinal permeability at D1 (*, $P < 0.05$) than WT mice. By D3 pi, while the FITC-dextran levels in *IEC-Myd88*$^{-/-}$ mice still were significantly higher than those of uninfected mice (**, $P < 0.005$) (Fig. 4A), they were no longer significantly higher than the levels in WT mice.

We next immunostained tissues for Ki-67, a nuclear factor marking cell proliferation (Fig. 4B), and noted similar levels of baseline IEC proliferation in uninfected WT and *IEC-Myd88*$^{-/-}$ mice. In contrast, at D1 pi, IEC proliferation was significantly

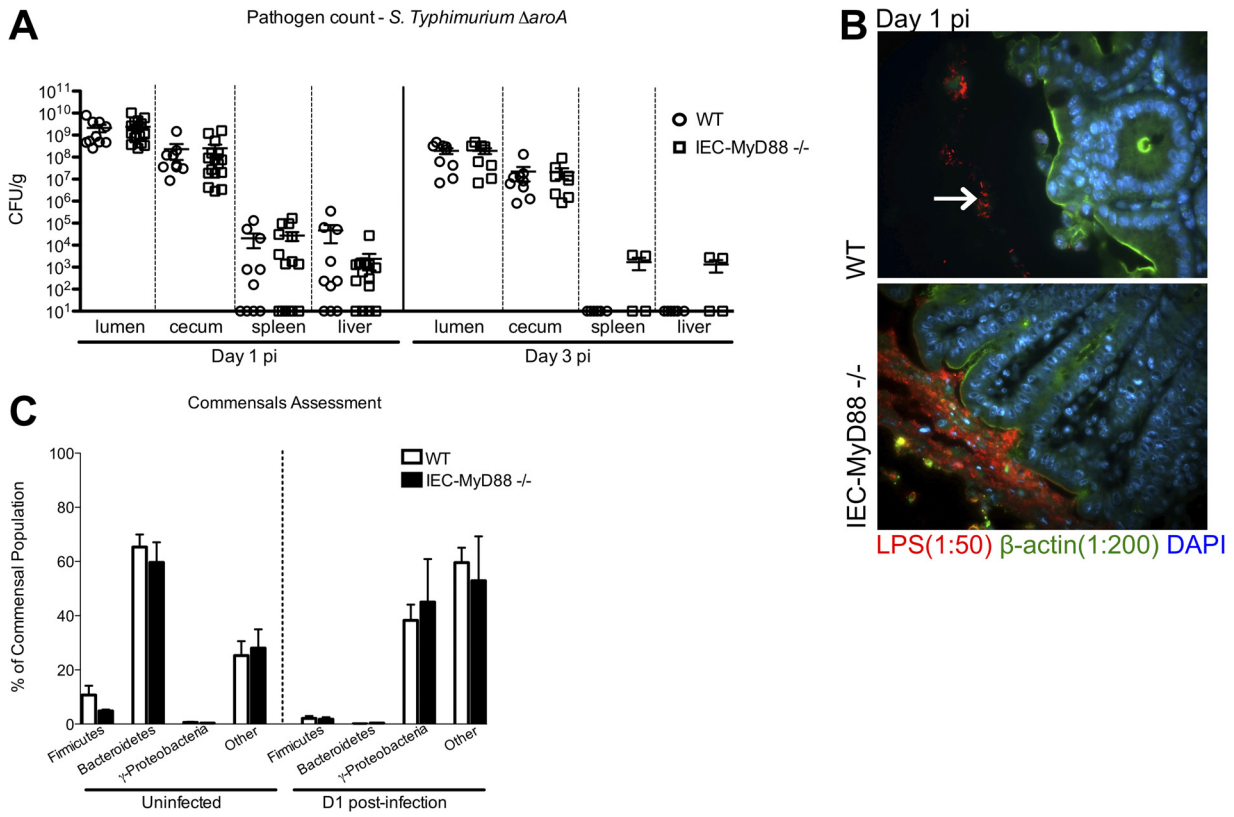

FIG 3 Disease severity of *IEC-MyD88*$^{-/-}$ mice is associated with altered *S.* Typhimurium localization within cecum. (A) No differences in *S.* Typhimurium Δ*aroA* mutant pathogen burdens (CFU/g) were identified among the ceca, luminal contents, spleens, or livers from *IEC-MyD88*$^{-/-}$ and WT mice at D1 or D3 pi. Error bars indicate SEM from at least 9 mice unless otherwise indicated. (B) Immunofluorescence staining for *Salmonella* LPS (red), β-actin (green), and DNA (blue) in cecal tissues at D1 pi. The presence of MyD88 in IECs (WT) prevents the *S.* Typhimurium Δ*aroA* mutant (location indicated by white arrow) from associating closely with the epithelium, sequestering them to the lumen, whereas *S.* Typhimurium in the *IEC-MyD88*$^{-/-}$ ceca was found in close proximity to the epithelial surface. Original magnification, ×200. (C) The commensal microbiota found in WT and *IEC-MyD88*$^{-/-}$ mice under uninfected conditions and after streptomycin treatment at D1 pi, as measured by qPCR. No significant differences were found between the intestinal bacterial populations (at phylum level) present in WT and *IEC-MyD88*$^{-/-}$ mice.

increased (measured as percent Ki-67-positive cells per crypt) in *IEC-Myd88*$^{-/-}$ crypts compared to WT crypts (***, $P < 0.0005$) (Fig. 4C). By D3 pi, IEC proliferation continued to increase in both groups, such that there were no significant differences between the two groups (Fig. 4C). These data indicate that MyD88 signaling within IECs plays a critical role in promoting protective barrier responses early during *S.* Typhimurium Δ*aroA* mutant infection. In contrast, MyD88 signaling within IECs is not required for the increased proliferation of IECs seen during infection, with the more rapid induction of proliferation in the *IEC-Myd88*$^{-/-}$ mice likely reflecting the accelerated inflammation these mice suffer.

IEC-Myd88$^{-/-}$ mice are impaired in antimicrobial and goblet cell-specific responses. While impaired IEC barrier function could help drive the exaggerated inflammation suffered by infected *IEC-Myd88*$^{-/-}$ mice, we examined whether there were other defects in IEC function/defense that could be involved. Interestingly, IEC-dependent MyD88 signaling previously has been found to maintain a microbial free zone above the host's mucosal surface in the small intestine (26). Upon assessment of several antimicrobial factors by qPCR, we found that they were expressed similarly in cecal tissues of the two mouse strains under uninfected conditions. As Vaishnava et al. (26) have previously reported a significant reduction of RegIII-γ gene transcript levels in the terminal ileum of uninfected *IEC-MyD88*$^{-/-}$ mice, we assessed its levels in the terminal ileum of our *IEC-MyD88*$^{-/-}$ mice and confirmed that compared to WT mice, RegIII-γ gene transcript levels in the ilea of *IEC-MyD88*$^{-/-}$ mice are impaired (data not shown). By D1 pi, transcription was significantly increased for several of these antimicrobial genes in WT mice; however, this induction was dramatically impaired for RegIII-γ (*, $P < 0.05$) (Fig. 5A) in the *IEC-Myd88*$^{-/-}$ mice. The induction of RegIII-β also seemed impaired, although the difference from WT mice did not reach significance.

Aside from antimicrobial factors, the mucosal surface of the large bowel is protected from luminal bacteria by a thick mucus layer that is largely comprised of the goblet cell-derived mucin Muc2. Therefore, we examined whether intrinsic MyD88 signaling affected goblet cell-specific factors. We assessed three goblet cell mediators, including Muc2, the proinflammatory mediator Relmβ, and the reparative trefoil factor 3 (TFF3). At the gene transcript level, all three were similar between *IEC-Myd88*$^{-/-}$ and WT mice under uninfected conditions. However, by D1 pi the transcript levels for all three factors were significantly lower in *IEC-Myd88*$^{-/-}$ mice than in WT mice (*, $P < 0.05$; **, $P < 0.005$) (Fig. 5B).

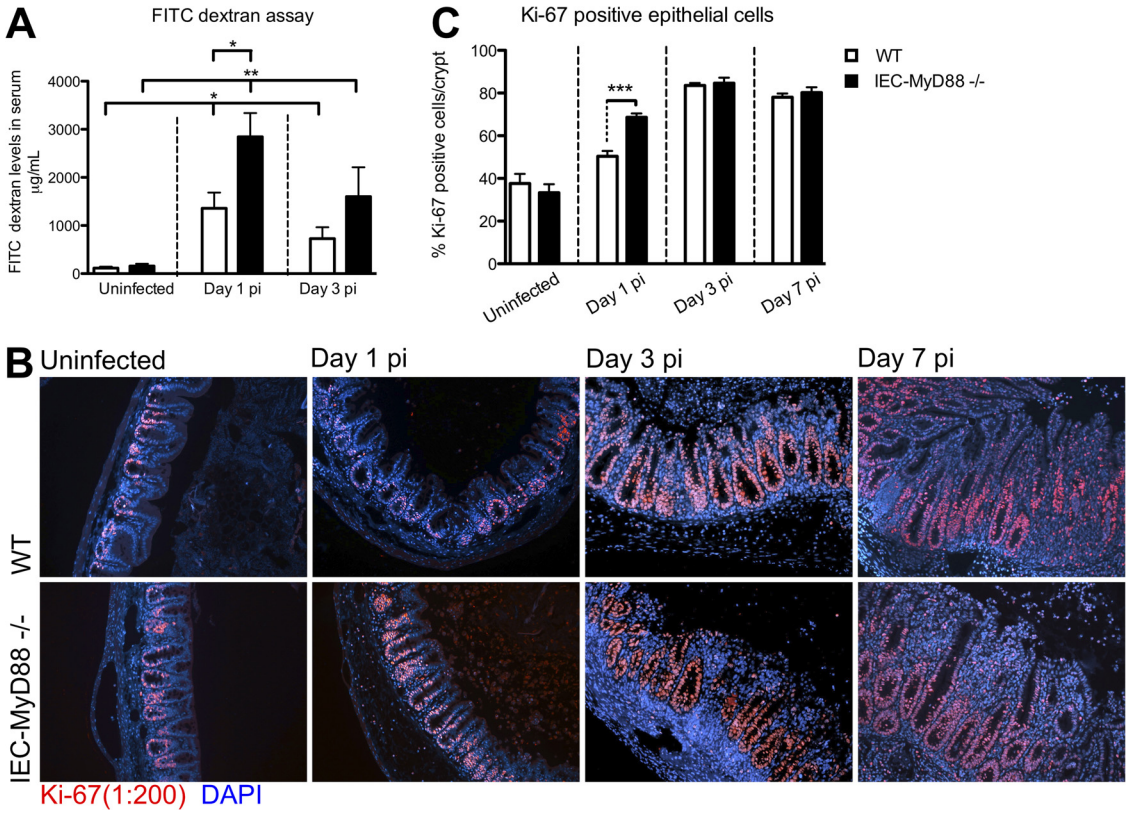

FIG 4 *IEC-MyD88*$^{-/-}$ mice display impaired barrier integrity at early infection time points. (A) FITC-dextran-based intestinal permeability assay performed on WT and *IEC-MyD88*$^{-/-}$ mice under uninfected as well as infected (D1 and D3 pi) conditions. *IEC-MyD88*$^{-/-}$ mice showed significantly increased barrier permeability compared to that of WT mice at D1 pi. Both groups experienced increased barrier permeability due to infection at D1 and D3 pi compared to that under uninfected conditions. Bars represent the average values for at least 7 mice per group from 3 or more independent experiments. *, $P < 0.05$; **, $P < 0.005$. (B) Immunostaining for the proliferation marker Ki-67 (red) and DNA (blue) revealed that WT and *IEC-MyD88*$^{-/-}$ mice had increased proliferation in cecal tissue beginning at D1 pi. (C) Quantification of percent Ki-67-positive cells per crypt showed there were significantly more proliferating cells in *IEC-MyD88*$^{-/-}$ mice at D1 pi than in WT mice.

Based on the impaired transcriptional induction of goblet cell-specific factors in *IEC-MyD88*$^{-/-}$ mice, along with the ability of Relmβ to induce antimicrobial genes (27), i.e., the RegIII proteins, and the role played by Muc2 in generating the protective mucus barrier (28), we wanted to further assess changes in these factors during infection. We used immunostaining to determine whether Relmβ and Muc2 were differentially expressed in the two mouse strains at the protein level during *S.* Typhimurium Δ*aroA* mutant infection. Whereas similar levels of Relmβ staining were seen in uninfected cecal tissues of WT and *IEC-MyD88*$^{-/-}$ mice (Fig. 6A), by D1 up to D7 pi there was a significant increase in detection of this protein within the goblet cells in WT mice (Fig. 6A), whereas there was little to no positive staining seen in tissues from infected *IEC-Myd88*$^{-/-}$ mice (Fig. 6A).

To semiquantify the expression of these proteins, Relmβ fluorescence intensity relative to that of DAPI in each section was assessed using the ImageJ integrated density analysis tool. By D1 pi, there was a 2-fold greater fluorescence intensity of Relmβ (relative to DAPI) in WT tissues than in *IEC-Myd88*$^{-/-}$ tissues. This increased to 6-fold by D3, which continued (and was significant) at D7 pi (Fig. 6C). Similarly, although comparable Muc2 staining was observed in uninfected WT and *IEC-Myd88*$^{-/-}$ tissues (Fig. 6B), by D1 up to D7 pi, WT tissues showed significantly increased Muc2 staining compared to that of *IEC-Myd88*$^{-/-}$ mice. Fluorescence intensity of Muc2 relative to that of DAPI was significantly greater in WT tissues at D1 pi (4-fold increase; *, $P < 0.05$) as well as at D3 (2-fold increase; **, $P < 0.005$) and D7 (2-fold increase; *, $P < 0.05$) pi (Fig. 6C).

IEC-Myd88$^{-/-}$ mice also show early susceptibility to *C. rodentium* infection. While our results clearly showed that *IEC-Myd88*$^{-/-}$ mice display increased susceptibility to early stages of *S.* Typhimurium infection, in an earlier study we found that MyD88 signaling within IECs played little role in regulating host responses to *C. rodentium* infection (15). Notably, the earliest time point we had studied with these mice was D6 pi. Therefore, we examined whether *IEC-Myd88*$^{-/-}$ mice showed any defects in promoting host defense against *C. rodentium* at an earlier time point, i.e., at D4 pi. Following euthanization and removal of the entire large bowel, *IEC-Myd88*$^{-/-}$ mice showed increased macroscopic damage in the form of shrunken ceca and shortened colons compared to WT mice (Fig. 7A). Interestingly, no differences in pathogen burdens were found between WT and *IEC-Myd88*$^{-/-}$ mice upon enumeration of *C. rodentium* in cecal tissue, luminal contents, and colonic tissues of infected mice (Fig. 7B).

To ensure consistency in our examination of responses, we once again focused our analysis on the cecum. Although the ceca of WT and *IEC-Myd88*$^{-/-}$ mice appeared similar under uninfected conditions, at D4 pi the *IEC-Myd88*$^{-/-}$ mice exhibited significantly in-

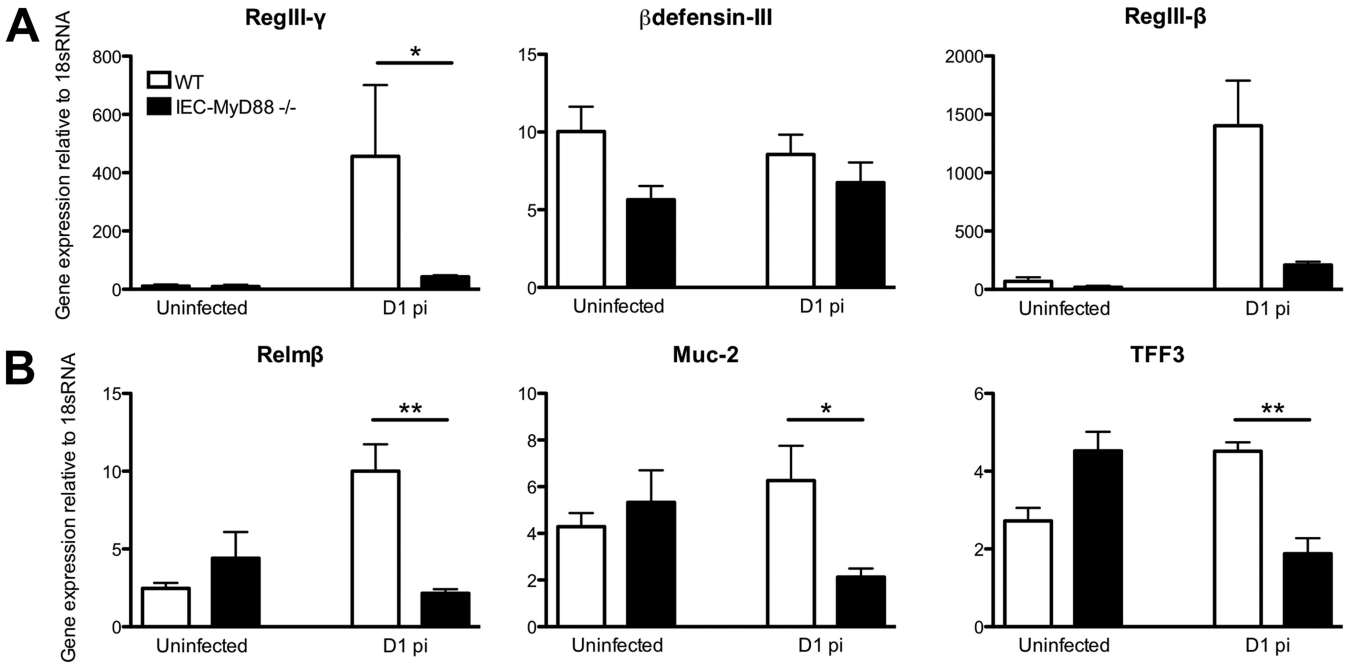

FIG 5 Infection-induced upregulation of gene transcripts for antimicrobial peptides and goblet cell mediators is impaired in *IEC-MyD88*$^{-/-}$ mice. (A) Infection of WT mice with the *S.* Typhimurium Δ*aroA* mutant led to increased gene transcript levels for RegIII-γ (significant) and RegIII-β (not significant) in cecal tissues by D1 pi compared to those of *IEC-MyD88*$^{-/-}$ mice. (B) *IEC-MyD88*$^{-/-}$ mice also were impaired in gene transcription levels in cecal tissues for the goblet cell mediators Relmβ, Muc2, and TFF3 at D1 pi compared to levels in WT mice. Error bars represent SEM from three independent experiments (at least 9 mice per group). *, $P < 0.05$; **, $P < 0.005$.

creased histological damage scores compared to WT mice (Fig. 7C and D). Specifically, *IEC-Myd88*$^{-/-}$ mice displayed increased crypt hyperplasia, edema, and greater inflammatory cell infiltration at D4 pi (Fig. 7D), but by D6 pi, pathology was similar between the two strains. FITC-dextran again was used to assess intestinal barrier permeability, and although there was a greater increase in FITC-dextran serum levels in *IEC-Myd88*$^{-/-}$ mice than in WT mice at D4 pi, it did not reach statistical significance (Fig. 8A).

Consistent with our assessment of *S.* Typhimurium infection, we next examined whether goblet cell-derived factors as well as antimicrobial responses were impaired in *IEC-Myd88*$^{-/-}$ mice during *C. rodentium* infection. Immunostaining revealed that at both D4 and D6 pi, WT tissues had greater Muc2-positive staining than *IEC-Myd88*$^{-/-}$ mice (Fig. 8B). To examine the effects of these changes on *C. rodentium* localization during infection, we stained tissues for the *C. rodentium* translocated effector *Tir*. In WT tissues, most *C. rodentium* organisms were found segregated within the cecal lumen at D4 pi; however, at the same time point in *IEC-Myd88*$^{-/-}$ mice, *C. rodentium* had successfully infected most of the cecal crypt epithelium (Fig. 8C).

Based on the impaired induction of goblet cell mediators and antimicrobial factors in *IEC-Myd88*$^{-/-}$ mice, as well as much closer epithelial association of bacteria during both *S.* Typhimurium and *C. rodentium* infection, we examined whether the antimicrobial activity at the intestinal mucosal surface was impaired in these mice. We isolated crypts from uninfected *IEC-Myd88*$^{-/-}$ and WT mice and collected their stimulated crypt supernatants to examine their bactericidal activity against the *S.* Typhimurium Δ*aroA* mutant and *C. rodentium*. As shown in Fig. 8D, relative to the growth of bacteria exposed to the negative control of iPIPES buffer alone, WT mouse crypt supernatants had direct bactericidal activity against *Salmonella* as well as *C. rodentium* (Fig. 8D), similar to that seen with purified RegIII-γ (positive control). When incubated with supernatants from *IEC-Myd88*$^{-/-}$ crypts, although some bactericidal activity was observed, it was significantly decreased against both bacterial strains compared to that of WT supernatants ($P < 0.0005$) (Fig. 8D). Thus, MyD88 signaling within IECs plays a key role in promoting antimicrobial defenses at the intestinal mucosal surface. Taken together, these results indicate that MyD88 signaling in IECs can actually determine host susceptibility to infection, potentially by controlling the ability of the pathogen to reach and survive at the surface of the intestinal epithelium and avoid subsequent accelerated intestinal tissue damage.

DISCUSSION

MyD88-dependent signaling previously has been shown to play a critical role in host defense against a number of bacterial pathogens (5, 6, 10); however, its role in the gastrointestinal tract appears to be unique, not only controlling pathogen burdens but also limiting pathogen access to mucosal tissues and limiting the tissue damage resulting from these infections. As many of these protective MyD88-dependent responses involve changes in the level of proliferation or function of the IEC layer, it was of significant interest to clarify whether these changes arose from intrinsic MyD88 signaling within the IECs themselves. In this study, we clearly showed that loss of MyD88 signaling in IECs leads to increased susceptibility to infection and to worsened intestinal tissue damage at the early stages of infection by two different bacterial pathogens. Mice lacking MyD88 signaling within their IECs were impaired in their ability to maintain barrier integrity or upregulate the expression of goblet cell or antimicrobial mediators during infection, allowing enteric pathogens to come into closer

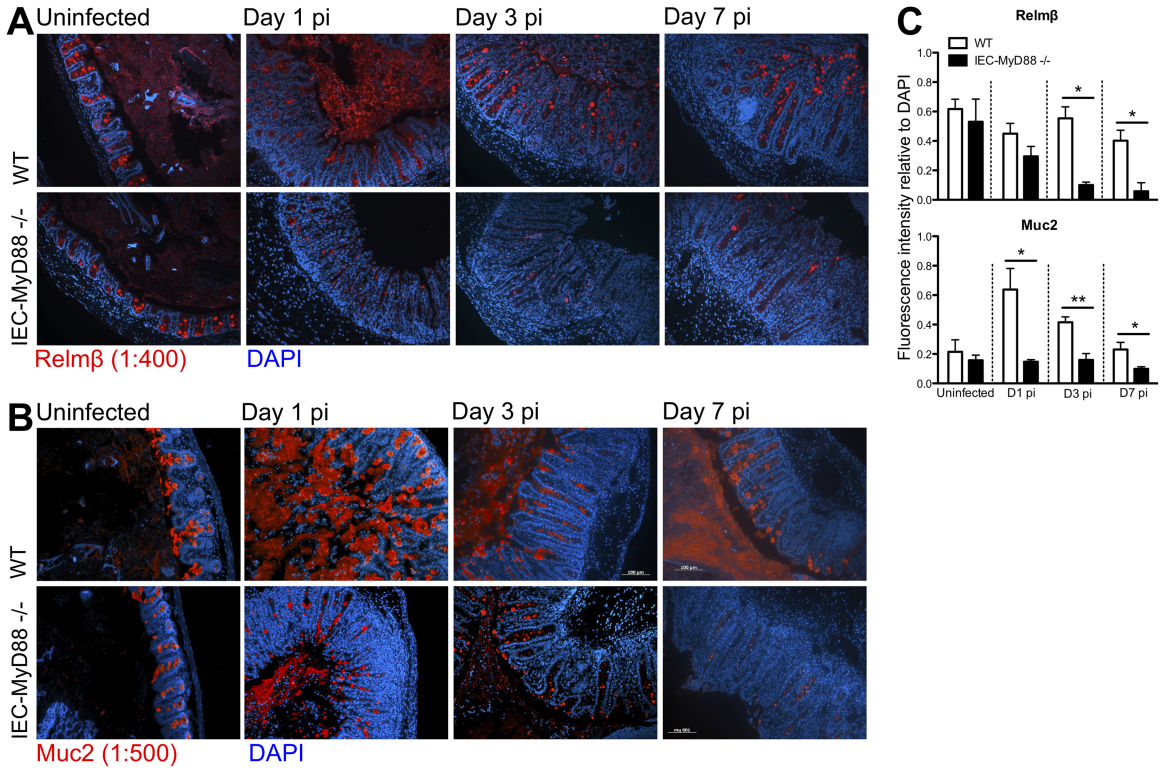

FIG 6 Muc2 and Relmβ production is impaired in infected *IEC-MyD88*$^{-/-}$ mice. (A and B) Representative immunostaining for the goblet cell-specific factors Relmβ (red) (A) and Muc2 (red) (B) in uninfected tissues and D1, D3, and D7 pi cecal tissues, with DNA stained in blue. (C) Fluorescence intensity measurements for Relmβ and Muc2 relative to total DNA staining using ImageJ software revealed WT tissues had significantly greater Relmβ- and Muc2-positive staining at D1, D3, and D7 pi. Bars represent the average fluorescence intensity values, with three measurements per mouse and at least 6 mice per group. *, $P < 0.05$; **, $P < 0.005$. Original magnification, ×200.

proximity with the intestinal epithelium and more rapidly cause infection. Through crypt-killing assays we found that crypts from mice lacking IEC-MyD88 signaling displayed significantly decreased antimicrobial capacity against both *S.* Typhimurium and *C. rodentium*. Thus, these findings expand our understanding of the role played by innate IEC signaling during *in vivo* enteric bacterial infections.

Several previous studies have shown that the global loss of MyD88 signaling in all cell types dramatically increased susceptibility of mice to colitis, leading to rapid mortality following induction of DSS or *C. rodentium* colitis (4–7). This susceptibility was found to reflect the loss of microbe-driven responses that promoted epithelial homeostasis and protection from epithelial injury. Striking defects observed in *Myd88*$^{-/-}$ mice included an inability to protect their IEC barrier function, resulting in exaggerated gut leakiness (4, 5). Moreover, these mice were unable to undergo the typical protective increases in colonic epithelial cell proliferation that develop during colitis, leaving them unable to readily replace damaged cells, resulting in widespread mucosal ulceration. In the current study, we clarify that at least in part, it is MyD88 signaling within the IECs themselves that protects/promotes IEC barrier function during infection, whereas this signaling is not required for the induction of increased IEC proliferation. In contrast, our results suggest that the proliferative status of IECs is driven by MyD88-dependent signaling by other cell types rather than IECs themselves.

There are three main subsets of IECs present within the large bowel, namely, enterocytes/colonocytes (80%), goblet cells (20%), and enteroendocrine cells (~1%). The intestinal epithelial monolayer acts as a physical barrier between the external environment, including the commensal microbes, and host tissues (13). In addition, a thick mucus layer is present, composed primarily of mucins secreted by GCs, which separates potentially hazardous luminal bacteria from the mucosal surface to avoid spontaneous and/or maladaptive inflammatory activation. The underlying enterocytes and goblet cells produce several types of antimicrobial peptides (RegIII-γ, β-defensin-III, RegIII-β, and mCRAMP) as well as tissue protective factors (Relmβ, Muc2, and TFF3). Many of these proteins are thought to localize within the overlying mucus layer as an optimal location to impact invading pathogens or repair damage to underlying tissues. At least in the small bowel, it has been shown that the mucus layer and the apical release of antimicrobials creates a sterile zone overlying the epithelium that helps limit contact between the microbiota and the epithelial barrier (26). Impaired function of this barrier, due to either reduced mucus production or dysfunctional antimicrobial responses, may allow bacteria to reach the epithelial surface where they can trigger detrimental and prolonged inflammatory responses. Our results suggest that MyD88 also regulates this zone of separation in the large bowel, at least during infection, and that in its absence, *S.* Typhimurium and *Citrobacter rodentium* were able to come into much closer association with the mucosal surface and more quickly invade tissues, causing more rapid tissue damage.

Our results noted overt impairment in the infection-induced ex-

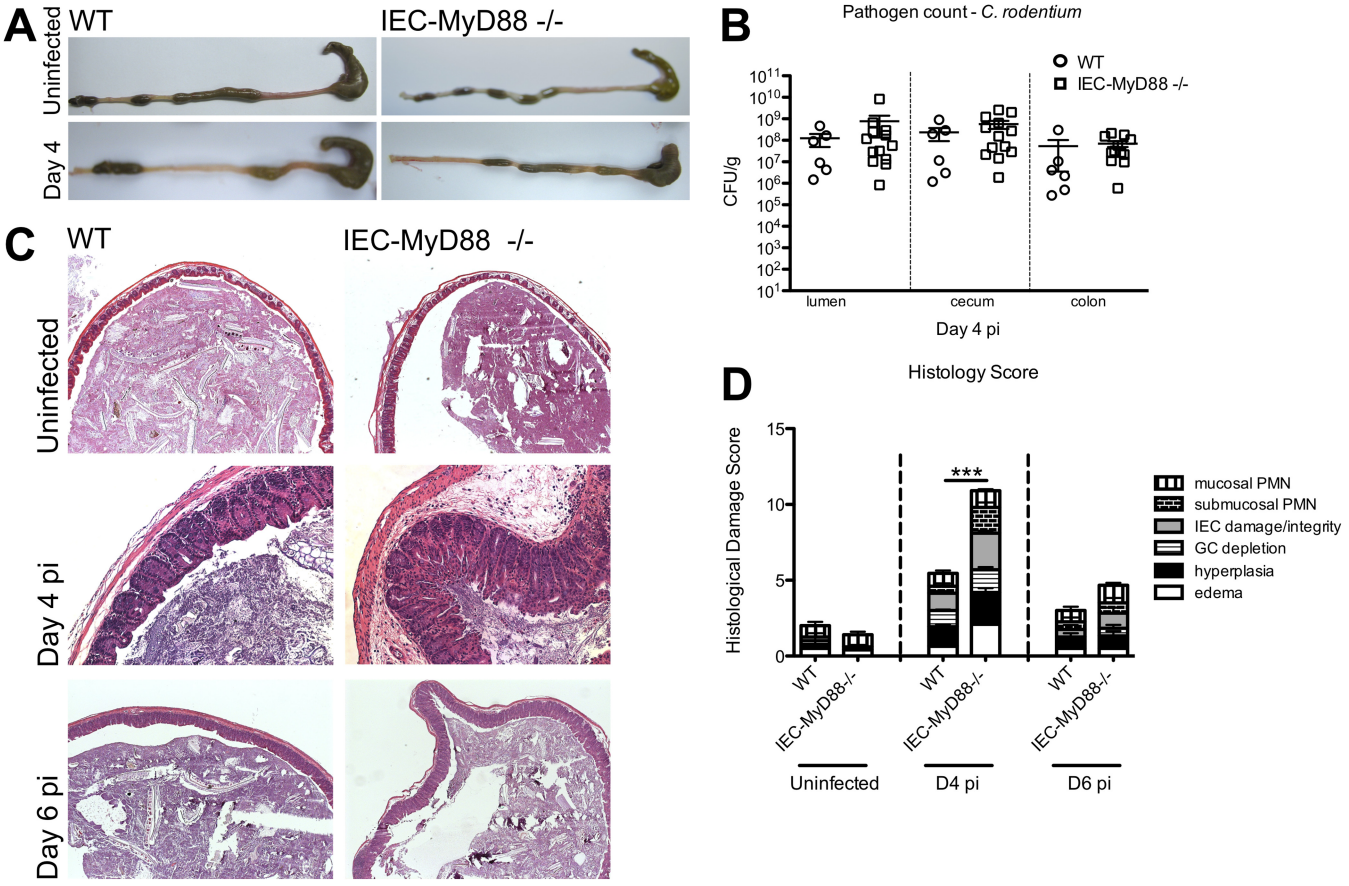

FIG 7 *IEC-MyD88*$^{-/-}$ mice suffer accelerated tissue damage during *C. rodentium* infection. (A) After *C. rodentium* infection, *IEC-MyD88*$^{-/-}$ mice displayed shrunken ceca compared to those of WT mice at D4 pi. (B) No differences in *C. rodentium* tissue pathogen burdens (CFU/g) were identified among the ceca, colons, or luminal contents from *IEC-MyD88*$^{-/-}$ and WT mice at D4 pi. Error bars indicate SEM from at least 6 mice. (C) Representative H&E staining of cecal tissues from D4 pi WT and *IEC-MyD88*$^{-/-}$ mice. *IEC-MyD88*$^{-/-}$ mice exhibit increased edema, hyperplasia, and damage to IEC integrity at D4 pi. (D) Comparative histological damage scores of uninfected and infected (D4 and D6 pi) *IEC-MyD88*$^{-/-}$ and WT mice. Cecal tissues of *IEC-MyD88*$^{-/-}$ mice had significantly higher histological damage scores at D4 pi. Bars represent the damage scores of at least 3 experiments, each with 3 to 5 mice. Error bars indicate SEM. ***, $P < 0.0005$.

pression of GC mediators in *IEC-Myd88*$^{-/-}$ mice compared to WT mice. At present, it is unclear whether these results indicate that MyD88 signaling in IECs preferentially controls GC responses or whether they are simply the easiest changes to detect in our system. As GCs have a secretory phenotype, immunohistochemical techniques allowed us to easily visualize the changes occurring in several GC-specific mediators; however, these techniques are not as easily employed to assess changes in antimicrobial factors. Future work using mice lacking MyD88 signaling within the goblet cell subset alone would aid in clarifying the role of GC MyD88-dependent innate signaling in conferring host susceptibility to infection.

It is also notable that IEC intrinsic MyD88 signaling appears to play a significant role in host defense only at early stages of infection. When we previously assessed the role of MyD88 signaling in IECs during *C. rodentium* infection at a later time point (D6 pi), we were unable to identify a significant defect in the protective host responses elicited during colitis (15). This was attributed to the previously described innate hyporesponsive status of IECs that is maintained by negative regulators, including Single Ig IL-1-related receptor (SIGIRR), a negative regulator of TLR and IL-1R signaling (14, 15). However, we report here that during the initial stages of enteric infection *in vivo*, MyD88 signaling within IECs plays a critical role in maintaining barrier integrity and limiting tissue damage through induction of several goblet cell-specific protective factors. We hypothesize that this early role for MyD88 signaling in IECs is lost at later time points due to increasing involvement of MyD88 signaling in infiltrating inflammatory cells, such as macrophages, which likely also regulate IEC proliferation and function.

Although we found no differences between WT and *IEC-Myd88*$^{-/-}$ mice under uninfected conditions, a recent study published by Frantz et al. reported baseline differences in the expression of RegIII-γ and Muc2 (16). Our inability to detect these differences may simply reflect differences in the commensal microbiota present in the different facilities. Correspondingly, Frantz et al. noted baseline differences in the commensal composition of *IEC-Myd88*$^{-/-}$ mice compared to WT mice after extensive and detailed analysis. They also observed a baseline increase in the translocation of commensal bacteria as well as compromised epithelial barrier integrity in the *IEC-Myd88*$^{-/-}$ mice. In contrast, we noted only modest differences in commensal composition between strains; using the FITC-dextran permeability assay, we

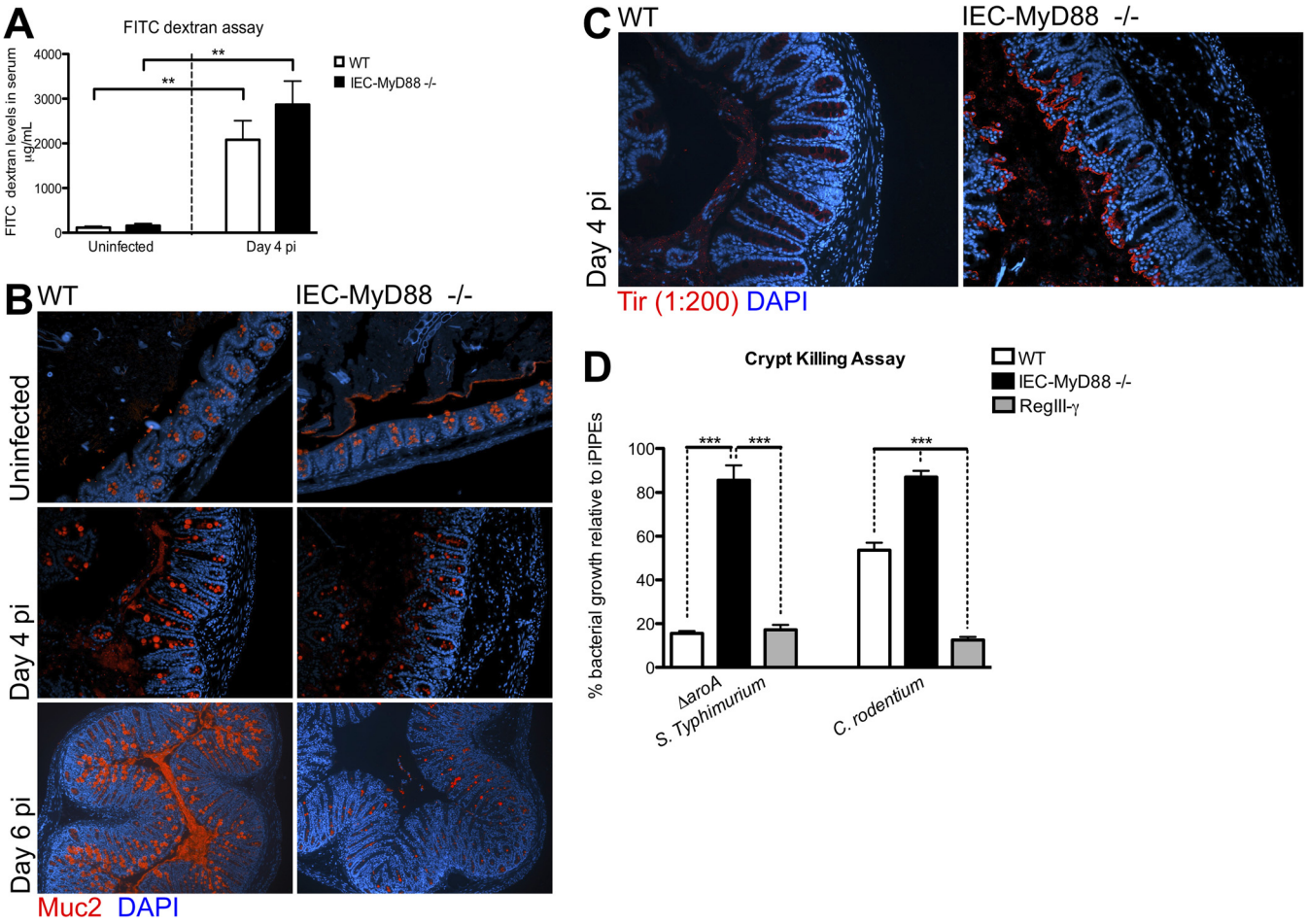

FIG 8 *IEC-MyD88*$^{-/-}$ mice show defects in Muc2 expression and crypt antimicrobial capacity. (A) Both WT and *IEC-MyD88*$^{-/-}$ mice experience increased barrier permeability at D4 pi. (B) Representative immunostaining for the goblet cell-specific factor Muc2 (red) in uninfected and infected (D4 and D6 pi) cecal tissues, with DNA stained blue. *IEC-MyD88*$^{-/-}$ mice have decreased positive Muc2 staining at D4 and D6 pi in cecal tissues compared to WT mice. (C) Immunostaining for the *C. rodentium* translocated effector Tir (red) and DNA (blue) at D4 pi reveals that the lack of MyD88 signaling in IECs allows *C. rodentium* to more readily infect cecal crypts than in WT mice, where they are sequestered to the lumen. (D) Cecal crypts isolated from WT mice possess greater bactericidal activity against the *S.* Typhimurium Δ*aroA* mutant and *C. rodentium* than crypts from *IEC-MyD88*$^{-/-}$ mice. Results are plotted as the average growth of bacteria relative to the negative-control iPIPES buffer (100% growth), with 20 μM RegIII-γ incubation presented as a positive control, and are representative of 2 independent experiments with 3 to 5 mice per group.

found similar barrier integrity in our *IEC-Myd88*$^{-/-}$ mice and WT mice. The lack of baseline differences noted in our facility may reflect our practice of cohousing *IEC-Myd88*$^{-/-}$ mice and WT (MyD88$^{flox/flox}$) mice upon bringing them into our facility (>10 generations cohoused), likely minimizing strain-specific differences in commensals.

In conclusion, our findings illuminate a novel role for IEC-specific MyD88 signaling in promoting host defense and tissue tolerance during early enteric infection, one that may have been overlooked previously due to the concept that IECs are innately hyporesponsive, particularly *in vivo*. We also demonstrate that MyD88 signaling may be more important in a certain subset of IECs, GCs, to limit significant early tissue damage, and we clarify which MyD88-dependent protective responses require IEC intrinsic signaling. Notably, although conflicting results on the innate responsive status of IECs *in vitro* have been reported (29–31), we show here for the first time that MyD88-dependent innate signaling within IECs actually can determine host susceptibility to an enteric bacterial infection.

ACKNOWLEDGMENTS

This work was supported by operating grants to B.A.V. from the Canadian Institutes of Health Research (CIHR) and the Crohn's and Colitis Foundation of Canada (CCFC). G.B. was supported by a CIHR MSc award, while both S.M.C. and G.B. were funded by University of British Columbia 4-year fellowships. M.S. was funded by a CIHR/CCFC/Canadian Association of Gastroenterology fellowship, while both V.M. and M.S. were funded by fellowships from the Michael Smith Foundation for Health Research. B.A.V. is the Children with Intestinal and Liver Disorders (CHILD) Foundation Chair in Pediatric Gastroenterology and the Canada Research Chair in Pediatric Gastroenterology.

The funders had no role in study design, data collection and analysis, decision to publish, or preparation of the manuscript.

REFERENCES

1. **Mandeville KL, Krabshuis J, Ladep NG, Mulder CJ, Quigley EM, Khan SA.** 2009. Gastroenterology in developing countries: issues and advances. World J. Gastroenterol. **15**:2839–2854. http://dx.doi.org/10.3748/wjg.15.2839.
2. **Ohl ME, Miller SI.** 2001. Salmonella: a model for bacterial pathogenesis.

Annu. Rev. Med. **52:**259–274. http://dx.doi.org/10.1146/annurev.med.52.1.259.

3. **Akira S, Takeda K.** 2004. Toll-like receptor signalling. Nat. Rev. Immunol. **4:**499–511. http://dx.doi.org/10.1038/nri1391.
4. **Rakoff-Nahoum S, Paglino J, Eslami-Varzaneh F, Edberg S, Medzhitov R.** 2004. Recognition of commensal microflora by Toll-like receptors is required for intestinal homeostasis. Cell **118:**229–241. http://dx.doi.org/10.1016/j.cell.2004.07.002.
5. **Gibson DL, Ma C, Bergstrom KSB, Huang JT, Man C, Vallance BA.** 2008. MyD88 signalling plays a critical role in host defence by controlling pathogen burden and promoting epithelial cell homeostasis during *Citrobacter rodentium*-induced colitis. Cell. Microbiol. **10:**618–631. http://dx.doi.org/10.1111/j.1462-5822.2007.01071.x.
6. **Lebeis SL, Bommarius B, Parkos CA, Sherman MA, Kalman D.** 2007. TLR signaling mediated by MyD88 is required for a protective innate immune response by neutrophils to *Citrobacter rodentium*. J. Immunol. **179:**566–577. http://dx.doi.org/10.4049/jimmunol.179.1.566.
7. **Araki A, Kanai T, Ishikura T, Makita S, Uraushihara K, Iiyama R, Totsuka T, Takeda K, Akira S, Watanabe M.** 2005. MyD88-deficient mice develop severe intestinal inflammation in dextran sodium sulfate colitis. J. Gastroenterol. **40:**16–23. http://dx.doi.org/10.1007/s00535-004-1492-9.
8. **Malvin NP, Seno H, Stappenbeck TS.** 2012. Colonic epithelial response to injury requires Myd88 signaling in myeloid cells. Mucosal Immunol. **5:**194–206. http://dx.doi.org/10.1038/mi.2011.65.
9. **Kirkland D, Benson A, Mirpuri J, Pifer R, Hou B, DeFranco AL, Yarovinsky F.** 2012. B cell-intrinsic MyD88 signaling prevents the lethal dissemination of commensal bacteria during colonic damage. Immunity **36:**228–238. http://dx.doi.org/10.1016/j.immuni.2011.11.019.
10. **Asquith MJ, Boulard O, Powrie F, Maloy KJ.** 2010. Pathogenic and protective roles of MyD88 in leukocytes and epithelial cells in mouse models of inflammatory bowel disease. Gastroenterology **139:**519–529. http://dx.doi.org/10.1053/j.gastro.2010.04.045.
11. **Brandl K, Sun L, Neppl C, Siggs OM, Le Gall SM, Tomisato W, Li X, Du X, Maennel DN, Blobel CP, Beutler B.** 2010. MyD88 signaling in nonhematopoietic cells protects mice against induced colitis by regulating specific EGF receptor ligands. Proc. Natl. Acad. Sci. U. S. A. **107:**19967–19972. http://dx.doi.org/10.1073/pnas.1014669107.
12. **Mundy R, MacDonald TT, Dougan G, Frankel G, Wiles S.** 2005. *Citrobacter rodentium* of mice and man. Cell Microbiol. **7:**1697–1706. http://dx.doi.org/10.1111/j.1462-5822.2005.00625.x.
13. **Goto Y, Kiyono H.** 2012. Epithelial barrier: an interface for the cross-communication between gut flora and immune system. Immunol. Rev. **245:**147–163. http://dx.doi.org/10.1111/j.1600-065X.2011.01078.x.
14. **Khan MA, Steiner TS, Sham HP, Bergstrom KSB, Huang JT, Assi K, Salh B, Tai IT, Li X, Vallance BA.** 2010. The single IgG IL-1-related receptor controls TLR responses in differentiated human intestinal epithelial cells. J. Immunol. **184:**2305–2313. http://dx.doi.org/10.4049/jimmunol.0900021.
15. **Sham HP, Yu EY, Gulen MF, Bhinder G, Stahl M, Chan JM, Brewster L, Morampudi V, Gibson DL, Hughes MR, McNagny KM, Li X, Vallance BA.** 2013. SIGIRR, a negative regulator of TLR/IL-1R signalling promotes microbiota dependent resistance to colonization by enteric bacterial pathogens. PLoS Pathog. **9**(8):e1003539. http://dx.doi.org/10.1371/journal.ppat.1003539.
16. **Frantz AL, Rogier EW, Weber CR, Shen L, Cohen DA, Fenton LA, Bruno MEC, Katzel CS.** 2012. Targeted deletion of MyD88 in intestinal epithelial cells results in compromised antibacterial immunity associated with downregulation of polymeric immunoglobulin receptor, mucin-2, and antibacterial peptides. Mucosal Immunol. **5:**501–512. http://dx.doi.org/10.1038/mi.2012.23.
17. **Chatfield SN, Strahan K, Pickard D, Charles IG, Hormaeche CE, Dougan G.** 1992. Evaluation of Salmonella typhimurium strains harbouring defined mutations in htrA and aroA in the murine salmonellosis model. Microb. Pathog. **12:**145–151. http://dx.doi.org/10.1016/0882-4010(92)90117-7.
18. **Wlodarska M, Willing B, Keeney KM, Menendez A, Bergstrom KS, Gill N, Russell SL, Vallance BA, Finlay BB.** 2011. Antibiotic treatment alters the colonic mucus layer and predisposes the host to exacerbated Citrobacter rodentium-induced colitis. Infect. Immun. **79:**1536–1545. http://dx.doi.org/10.1128/IAI.01104-10.
19. **Layton A, McKay L, Williams D, Garrett V, Gentry R, Sayler G.** 2006. Development of bacteroides 16S rRNA gene TaqMan-based real-time PCR assays for estimation of total, human, and bovine fecal pollution in water. Appl. Environ. Microbiol. **72:**4214–4224. http://dx.doi.org/10.1128/AEM.01036-05.
20. **Guo X, Xia X, Tang R, Zhou J, Zhao H, Wang K.** 2008. Development of a real-time PCR method for Firmicutes and Bacteroidetes in faeces and its application to quantify intestinal population of obese and lean pigs. Lett. Appl. Microbiol. **47:**367–373. http://dx.doi.org/10.1111/j.1472-765X.2008.02408.x.
21. **Bacchetti De Gregoris T, Aldred N, Clare AS, Burgess JG.** 2011. Improvement of phylum- and class-specific primers for real-time PCR quantification of bacterial taxa. J. Microbiol. Methods **86:**351–356. http://dx.doi.org/10.1016/j.mimet.2011.06.010.
22. **Fierer N, Jackson JA, Vilgalys R, Jackson RB.** 2005. Assessment of soil microbial community structure by use of taxon-specific quantitative PCR assays. Appl. Environ. Microbiol. **71:**4117–4120. http://dx.doi.org/10.1128/AEM.71.7.4117-4120.2005.
23. **Hirota SA, Ng J, Lueng A, Khajah M, Parhar K, Li Y, Lam V, Potentier MS, Ng K, Bawa M, McCafferty DM, Rioux KP, Ghosh S, Xavier RJ, Colgan SP, Tschopp J, Muruve D, MacDonald JA, Beck PL.** 2011. NLRP3 inflammasome plays a key role in the regulation of intestinal homeostasis. Inflamm. Bowel Dis. **17:**1359–1372. http://dx.doi.org/10.1002/ibd.21478.
24. **Valdez Y, Grassl GA, Guttman JA, Coburn B, Gros P, Vallance BA, Finlay BB.** 2009. Nramp1 drives an accelerated inflammatory response during Salmonella-induced colitis in mice. Cell Microbiol. **11:**351–362. http://dx.doi.org/10.1111/j.1462-5822.2008.01258.x.
25. **Barthel M, Hapfelmeier S, Quintanilla-Martinez L, Kremer M, Rohde M, Hogardt M, Pfeffer K, Rüssman H, Hardt WD.** 2003. Pretreatment of mice with streptomycin provides a *Salmonella enterica* serovar Typhimurium colitis model that allows analysis of both pathogen and host. Infect. Immun. **71:**2839–2858. http://dx.doi.org/10.1128/IAI.71.5.2839-2858.2003.
26. **Vaishnava S, Yamamoto M, Severson KM, Ruhn KA, Yu X, Koren O, Ley R, Wakeland EK, Hooper LV.** 2011. The antibacterial lectin RegIII-γ promotes the spatial segregation of microbiota and host in the intestine. Science **334:**255–258. http://dx.doi.org/10.1126/science.1209791.
27. **Hogan SP, Seidu L, Blanchard C, Groschwitz K, Mishra A, Karow ML, Ahrens R, Artis D, Murphy AJ, Valenzuela DM, Yanopoulos G, Rothenberg ME.** 2006. Resistin-like molecule beta regulates innate colonic function: barrier integrity and inflammation susceptibility. J. Allergy Clin. Immunol. **118:**257–268. http://dx.doi.org/10.1016/j.jaci.2006.04.039.
28. **Zarepour M, Bhullar K, Montero M, Ma C, Huang T, Velcich A, Xia L, Vallance BA.** 2013. The mucin Muc2 limits pathogen burdens and epithelial barrier dysfunction during Salmonella enterica serovar Typhimurium colitis. Infect. Immun. **81:**3672–3683. http://dx.doi.org/10.1128/IAI.00854-13.
29. **Melmed G, Thomas LS, Lee N, Tesfay SY, Lukasek K, Michelsen KS, Zhou Y, Hu B, Arditi M, Abreu MT.** 2003. Human intestinal epithelial cells are broadly unresponsive to Toll-like receptor 2-dependent bacterial ligands: implications for host-microbial interactions in the gut. J. Immunol. **170:**1406–1415. http://dx.doi.org/10.4049/jimmunol.170.3.1406.
30. **Otte JM, Cario E, Podolsky DK.** 2004. Mechanisms of cross hyporesponsiveness to Toll-like receptor bacterial ligands in intestinal epithelial cells. Gastroenterology **126:**1054–1070. http://dx.doi.org/10.1053/j.gastro.2004.01.007.
31. **Cario E, Rosenberg IM, Brandwein SL, Beck PL, Reinecker HC, Podolsky DK.** 2000. Lipopolysaccharide activates distinct signaling pathways in intestinal epithelial cell lines expressing Toll-like receptors. J. Immunol. **164:**966–972. http://dx.doi.org/10.4049/jimmunol.164.2.966.